2004

Thermal Expansion Prediction of Compressor Piston

Mario Lavella
Politecnico di Torino

Paolo Valero
Embraco Europe

Roberto Doglione
Politecnico di Torino

Marek Zgliczynski
Embraco Europe

THERMAL EXPANSION PREDICTION OF COMPRESSOR PISTON

Mario LAVELLA [1], Paolo VALERO [2], Roberto DOGLIONE [3], Marek ZGLICZYNSKI [4]

[1]Politecnico di Torino,
C.so Duca degli Abruzzi, 24 – 10129 Turin - Italy
Phone +39 011 5644612 – Fax +39 011 5644699 - E-mail mario.lavella@polito.it

[2]Embraco Europe,
Via Buttigliera, 6 – 10020 Riva presso Chieri (To) - Italy
Phone +39 011 9437599 – Fax +39 011 9437397 - E-mail paolo.valero@embraco.it

[3]Politecnico di Torino,
C.so Duca degli Abruzzi, 24 – 10129 Turin - Italy
Phone +39 011 5644612 – Fax +39 011 5644699 - E-mail roberto.doglione@polito.it

[4]Embraco Europe,
Via Buttigliera, 6 – 10020 Riva presso Chieri (To) - Italy
Phone +39 011 9437301 – Fax +39 011 9437397 - E-mail marek.zgliczynski@embraco.it

ABSTRACT

The paper deals with the thermal expansion of pistons for refrigeration compressors, that were in the past of gray cast iron, but presently are made of sintered steel.. The design must ensure the compatibility of components thermal expansion to obtain correct gap between piston and cylinder, both for performance and reliability reasons.
Sintered steel parts have a broad range of porosity distribution, according to the pressure distribution during the powder pressing. The overall elastic and thermal properties of the sintered piston were estimated by combining the properties of each constituent (ferrite, pearlite, void, magnetite). The local constituent volume fraction was measured by quantitative metallographic analysis.
To predict steady-state thermal dilatations, the thermo-mechanical modeling was carried out by a simplified coupling between structure and thermal-fluid, using overall heat transfer coefficients estimated at average temperature and velocity conditions.

1. INTRODUCTION

In refrigeration reciprocating compressors, piston is not using elastic split rings, but the leakage in compression chamber is controlled by means of the high precision coupling between piston and cylinder bore, with a diametrical clearance of few microns. While compressor is running, the differential thermal expansion between sintered piston and cast iron cylinder can modify the correct clearance, causing performances decreasing, oil circulation increasing, abnormal wear and even compressor seizing.
Cast iron piston, because structure homogeneity and affinity to cylinder material, offers optimal behaviour . Recently is diffused the use of sintered steel pistons, because of advantages in manufacturing process and compressor efficiency. Material non homogeneity, intrinsically related to powders pressing process, is causing a non uniform thermal dilatation. The oxprot process for surface sealing, creating a different oxide concentration, is even increasing this effect, because also material composition is not uniform.

By means of a thermo-mechanical model, the thermal expansion of the piston in steady state conditions can be predicted, and acting on piston design, the distortion of the original shape can be minimized to obtain reliability and performances equivalent to cast iron piston.
Preliminary to the calculation activity, the thermal and elastic characteristics of sintered steel, in three different parts of the piston, have been evaluated by means of metallographic analysis on a statistically significant number of sections. The overall characteristics has been then obtained using mixtures rule and micromechanics concepts.

2. SINTERED STEEL PHYSICAL CHARACTERISTICS

Sintered steel is C-Mn-S type, and its chemical composition is shown in Table 1. The high carbon content has the purpose of making thermal elongation similar to crankcase, made of cast iron.

Table 1: chemical composition (% by weight) of sintered steel

C	Mn	S	Fe	MnS
0,6	0,4	0,16	bal.	0,55

The microstructural components are ferrite, pearlite, manganese sulfide and voids. Manganese sulfide, useful to improve machinability, will be disregarded because of its small amount.
The machined piston is subjected to oxprot treatment, consisting in heating in oven with water vapor , with the purpose of sealing part surfaces with a layer of few microns of magnetite ($Fe_3O_{4)}$. Because of high interconnected porosity of the sintered steel, the vapor is diffusing in the depth of the material and a significant amount of magnetite is constituted also inside the piston, especially along the sides.
For the purposes of this study, the sintered piston is assumed to consist of three phases: the steel matrix (containing ferrite and cementite), the magnetite (Fe_3O_4) and the voids. Relevant characteristics are the Young modulus **E**, the Poisson coefficient n, the thermal expansion coefficient a, the thermal conductivity coefficient **k**.

For voids, all characteristics are considered null:
$\mathbf{E_v}$, n_v, a_v, $\mathbf{k_v=0}$.
For steel matrix, elastic properties are as standard steel, because working temperature is around 100°C. Thermal properties (a and **k**) are got from Smithells [1], interpolating the data for carbon content of 0,6%:
$\mathbf{E_a=207\ Gpa}$, $n_a=0,3$, $a_a=12,65\times10^{-6}\ K^{-1}$, $k_a=46,7\ Wm^{-1}K^{-1}$.
About magnetite, this ceramic material is commonly used for magnetic applications, but it's not easy to find out informations about elastic and thermal characteristics. Reference sources are [2, 3]:
$\mathbf{E_m=200\ Gpa}$, $n_m=0,3$, $a_m=6\times10^{-6}\ K^{-1}$, $k_m=5\ Wm^{-1}K^{-1}$.

3. SINTERED PISTON PHYSICAL CHARACTERISTICS

The global properties of a multiphase material can be directly measured, or calculated as a combination of single phases properties. The main parameter that influences material behaviour is the density, related to local porosity and composition. Porosity of sintered steel is continuously varying along the component, but for sake of simplicity we have considered three different cases: 1) piston top, 2) piston side in thin section, 3) piston side in thick section.
It is obvious that a direct measure of the properties should be preferable, but the porosity gradients in the piston (Figure 1) imposes constraints on the dimensions of the samples. To obtain reliable results, very small samples should be used, the biggest size less than a millimeter. Some attempt was made to measure the thermal elongation coefficient, but it was impossible to use specimens smaller than 3 mm. The results were scattered and inconsistent.
It was then decided to estimate the properties by calculations, using micromechanics guidelines. Each zone of the piston was analyzed by quantitative metallography to obtain the local percentage of the phases. From 10 to 20 samples were taken for each observed zone.

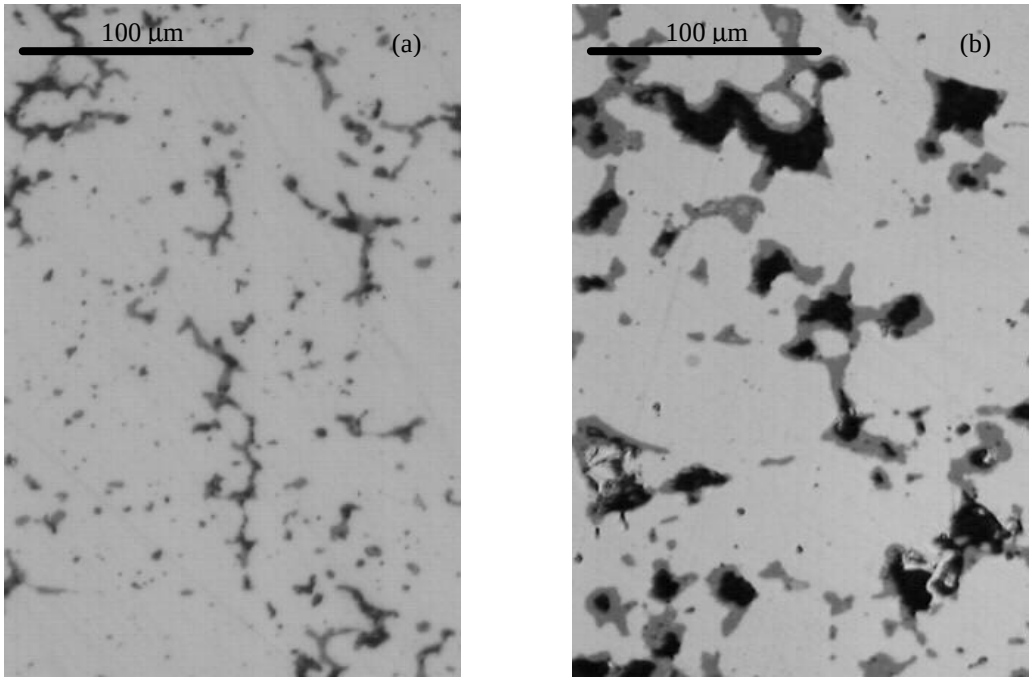

Figure 1: microstructure of piston top (a) and side in thin section (b); light gray is steel matrix, black zones are voids, dark gray areas are magnetite created by oxprot treatment.

Area fractions of each constituent, for a well known stereology theorem, are corresponding to volume fractions of microstructural components. Results of the measurements, averaged for each relevant zone, are shown in Table 2.

Table 2: microstructural constituents composition obtained with metallographic analysis (s is standard deviation).

Component (% volume)	Piston top (s =1,3%)	Piston thin side (s =3,1%)	Piston thick side (s =3,6%)
Steel	90,63	74,5	82,11
Fe_3O_4	8,07	17,23	11,45
Void	1,3	8,27	6,47

It's evident the difference between piston top, with a higher percentage of metallic matrix, and piston sides, with a larger amount of voids and magnetite, due to powders pressing and oxprot processes. The average density in the three parts of the piston can be estimated applying the rule of mixture shown in equation (1):

$$r = \sum_{i=1}^{3} r_i x_i \qquad (1)$$

where r_i is the density and $\mathbf{x_i}$ is volume fraction of each component. Results are shown in Table 3.

Table 3: density of constituents and different piston regions

Constituent or region	Steel C60	Magnetite Fe_3O_4	Void	Piston top	Piston thin side	Piston thick side
density [Kg/m^3]	7850	5200	0	7534	6744	7041

Defined the constituents volume fraction and the density of each piston region, it's now possible to estimate all elastic and thermal properties. Using experimental data for sintered steel without oxprot treatment [4] for **E**, n ed a, empirical relationship published in literature for a and **k** [5, 6], and finally interpolating for the density interval of interest, we have applied the mixture rule and obtained values shown in Table 4.

Table 4: calculated properties of sintered piston with oxprot treatment by application of mixtures rule.

	Piston top	Piston thin side	Piston thick side
E [Gpa]	203	189	193
ν	0,3	0,28	0,28
α [°K^{-1}]	$11{,}95\cdot10^{-6}$	$10{,}46\cdot10^{-6}$	$11{,}07\cdot10^{-6}$
k [W/mK]	42,7	35,7	38,9

Magnetite effect is important, but is probably overestimated using mixture rule: magnetite thermal expansion is smaller than that of steel matrix, producing a compression effect that is reducing its expansion [7]. As consequence, the global thermal expansion coefficient will be smaller than the result of mixture rule application. The physical reality will be intermediate between values obtained by the application of mixture rule and values obtained by interpolating experimental data [4] and using empirical relationships [5, 6] disregarding magnetite presence. Thus, the final values used for the numerical calculations reported in the next paragraphs are shown in Table 5.

Table 5: estimated properties of sintered piston with oxprot treatment.

	Piston top	Piston thin side	Piston thick side
E [Gpa]	180	150	160
ν	0,28	0,24	0,26
α [°K^{-1}]	$11{,}18\cdot10^{-6}$	$9{,}83\cdot10^{-6}$	$10{,}44\cdot10^{-6}$
k [W/mK]	42,7	35,7	38,9

4. THERMAL AND MECHANICAL MODEL

The main aim of this section is to define a model that shows the different piston behaviour between a uniform material and a sintered steel with not uniform porosity, when the compressor works in thermal steady state. In other words, we want to correlate the thermal steady state elongation with the porosity generated by sintering process of the piston, using two models, first based on an axisymmetric geometry, second based on a three-dimensional geometry. The scheme of the axisymmetric geometry is shown in figure 2.

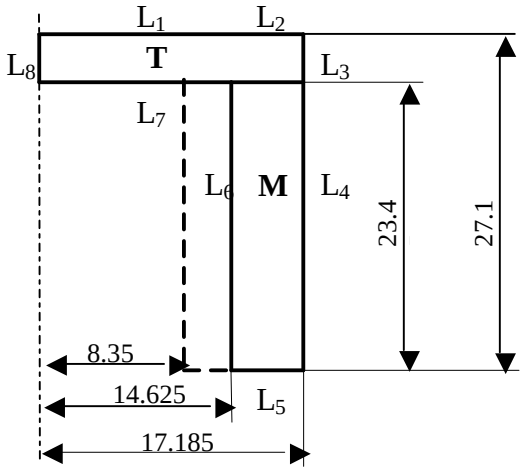

Figure 2: geometry [mm] used for axisymmetric calculation,
the symbols T and M referring respectively to piston top and piston side.

The thermal loads on the piston depend on the thermal exchange of the piston surface with the compressed fluid, the fluid contained in compressor shell, and on friction heat generated on the lateral surface (L_3 and L_4 in figure 2) of the

piston. The hypothesis used to estimate the thermal loads are: radiation exchange and friction heat may be neglected; the surface L_1 L_2 exchanges heat by convection with fluid at uniform temperature Ta; the surface L_5 L_6 L_7 exchanges heat by convection with fluid at uniform temperature Tc. The thermal model originated from the previous hypothesis can be written in the form:

$$\mathrm{div}(k \cdot \mathbf{grad}(T)) = 0 \tag{2}$$

$$-k \cdot \mathbf{grad}(T) \cdot \mathbf{n} = h_a (T_s - T_a)\text{; on } L_1\ L_2 \tag{3}$$

$$-k \cdot \mathbf{grad}(T) \cdot \mathbf{n} = h_c (T_s - T_c)\text{; on } L_5\ L_6\ L_7 \tag{4}$$

$$-k \cdot \mathbf{grad}(T) \cdot \mathbf{n} = 0\text{; on } L_3\ L_4\ L_8 \tag{5}$$

where the symbols refer to: T temperature point by point in the piston; k thermal conductivity; **n** normal unit vector to surface; T_s surface temperature; Ta average temperature of the compressed fluid during the working cycle; h_a convection coefficient between fluid and surfaces L_1 L_2; Tc average temperature of the fluid contained in the compressor lower during the working cycle; h_c convection coefficient between fluid and surfaces L_5 L_6 L_7. This coefficient has been estimated using classical dimensionless correlation between the thermophysical property of the fluid and the characteristic flow velocity (e.g. Perry, 1997).

The mechanical model is based on the stress strain balance equation for axisymmetric geometry. The constitutive law used is the linear isotropic thermo-elasticity following:

$$\varepsilon = \varepsilon^{el} + \varepsilon^{th} \tag{7}$$

where ε^{el} is the elastic strain and ε^{th} is the thermal strain. The mentioned strain are given by:

$$\varepsilon^{el}_{i,j} = \frac{1+\nu}{E}\sigma_{ij} - \frac{\nu}{E}\sigma_{kk}\delta_{ij} \tag{8}$$

$$\varepsilon^{th} = \alpha \cdot T \tag{9}$$

where E is the Young's modulus, ν is the Poisson's ratio, σ is the stress, α is the expansion coefficient, δ_{ij} is the Kronecher's symbol, and i,j,k can assume the complete value (1, 2, 3).

The thermo-mechanical properties (k, E, ν, α) used in the calculation are function of geometry in order to take in count the effect of the porosity of the sintered steel. Particularly this property has been distinguished in two region of the piston respectively indicate with T and M in figure 2.

5. RESULTS AND DISCUSSION

Several different combinations of geometry and thermo-mechanical properties have been analysed with axisymmetric geometry, considering both the uniform material and the different thermo-mechanical properties of sintered steel as a function of the geometry.
The figure 3 shows the isotherms at steady state in the two above cases, for thin piston side: in the case (a) are considered two different values of the thermal conductivity for piston top and lateral side while the case (b) takes in count a unique value for all geometry. In steady state condition the thermal gradients are lower than 0.5°C. A similar situation occurs in the cases, not shown in the paper, with piston thick side. Such behaviours are due to low convection coefficient and low difference of temperature between the compressed fluid and fluid contained in compressor shell. Consequently the thermal stresses are very low, the temperature of the piston is around 100 °C, and the effect of porosity of sintered steel absolutely negligible on temperature distribution.

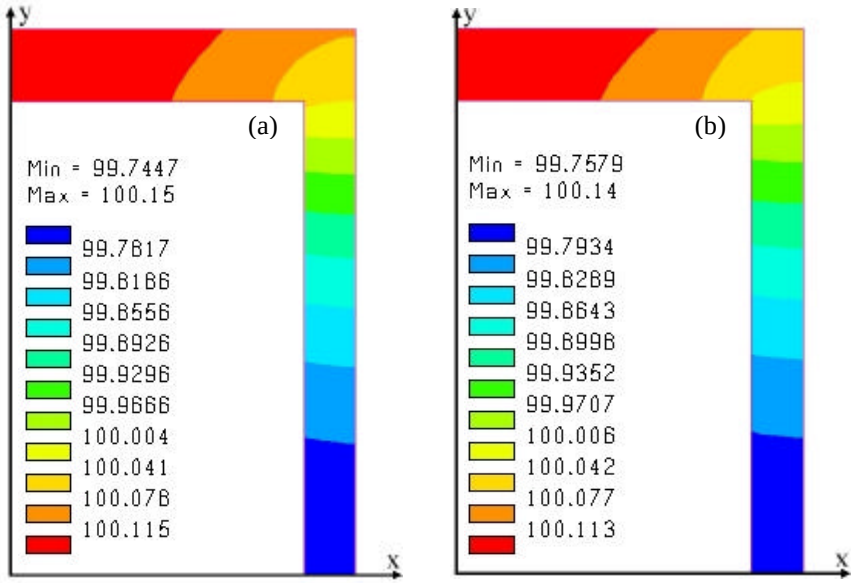

Figure 3: isotherms [°C] obtained (a) considering thermal conductivity as a function of geometry and (b) considering a single averaged value in all geometry.

The figure 4 shows the results of thermo-mechanical computation relative to thermal distribution of figure 3 considering (a) different thermo-mechanical properties as a function of the geometry and (b) thermo-mechanical properties homogeneous in all the geometry. It's evident that mechanical elongation is strongly dependent on the thermo-mechanical properties of different piston parts.

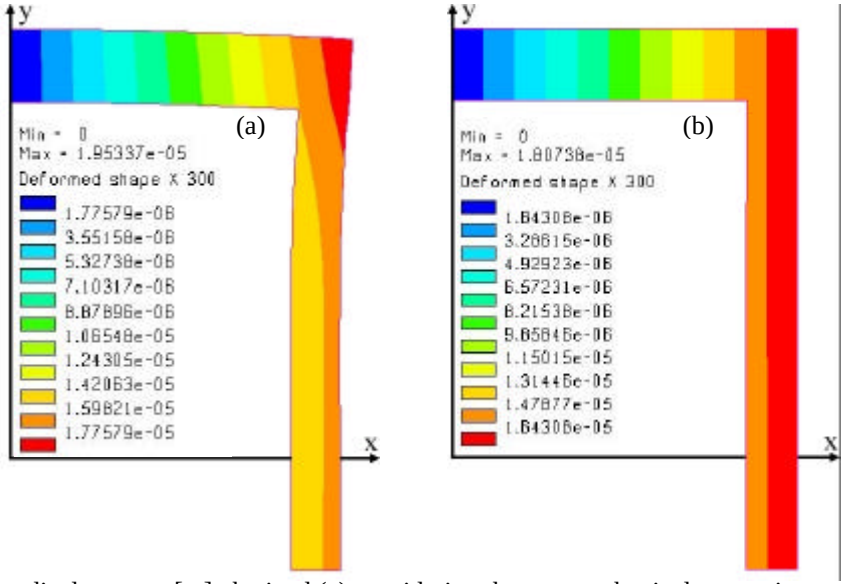

Figure 4: x-direction displacement [m] obtained (a) considering thermo-mechanical properties as a function of geometry and (b) considering a single averaged value in all the geometry.

The deformed shape obtained considering thermo-mechanical properties as a function of geometry is conical while the deformed shape of homogeneous material is cylindrical. This difference of behaviour is due to different value of expansion coefficient assumed for the piston top and the piston side, related to porosity gradient and material composition (see figure 1). In the cases of geometry with lateral side thick the behaviour is similar but is slightly more conical (about 1%).

The figure 5 shows the thermo-mechanical displacement in the radial direction obtained applying the expansion coefficient as a function of geometry with the value of table 5. Moreover this computational result do not to keep count of thermal gradients. In other words it is based on the hypothesis that the piston at steady state reaches a uniform temperature in each point of its geometry. The uniform temperature is achieved in steady state and average constant heat flux between two source (heat and cold respect to piston) with low convection coefficient and difference of temperature. In fact the results of the figure 3 shows that the thermal gradient is negligible.

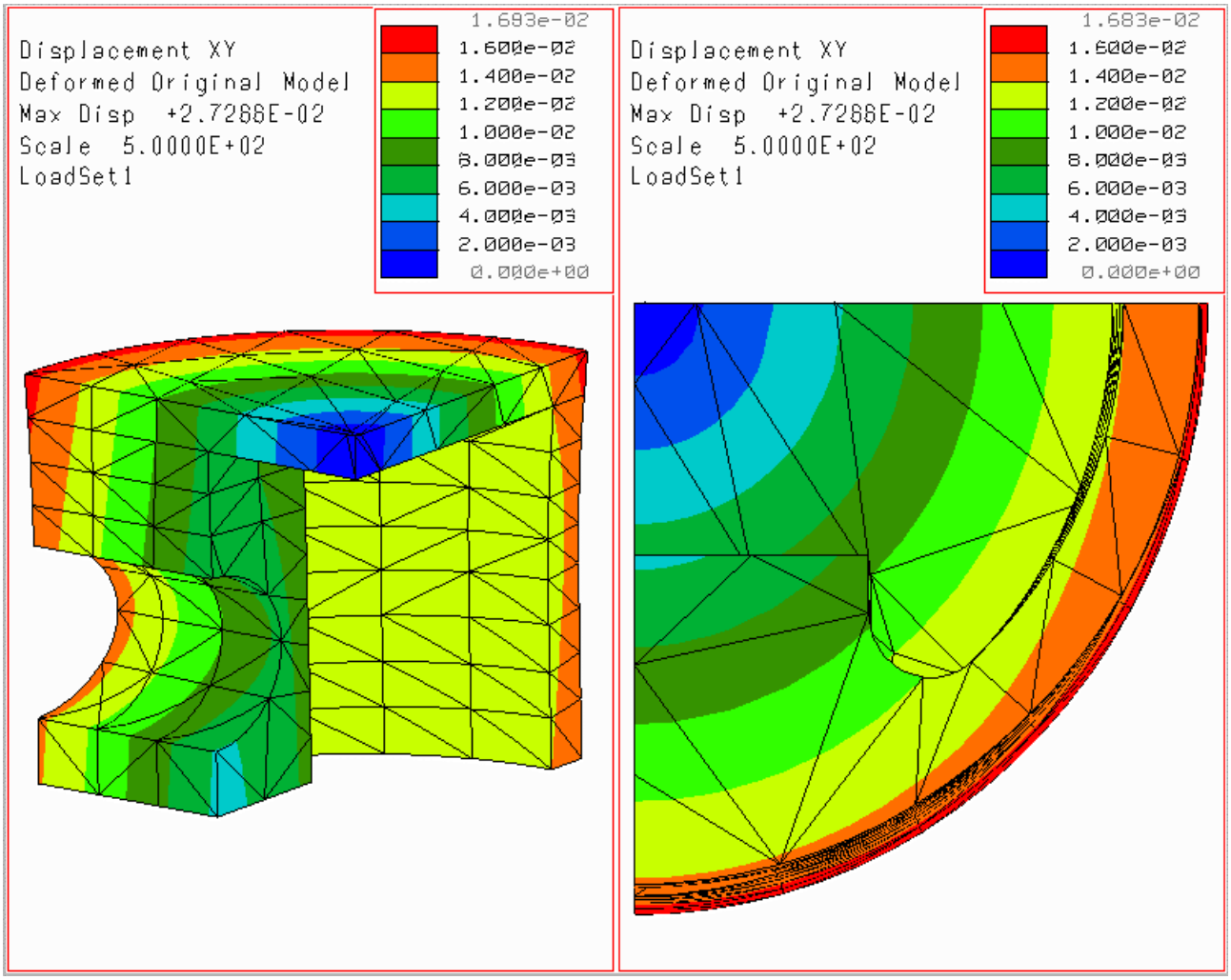

Figure 5: thermo-mechanical displacement [mm] in the radial-direction
obtained considering the thermo-mechanical properties as a function of geometry.

The three-dimensional deformed shape is coherent with the axisymmetric analysis. Actually it shows the conical shape in vertical direction that we have seen in axisymmetric model and an elliptical shape in top view with longest axis parallel to piston pin hole. The elliptical shape of the piston lower side is more conical than piston top because the holes to interrupt the coherences of the strain respect to top of the piston.

8. CONCLUSIONS

The volume fraction of sintered steel type C-Mn-S has been obtained by quantitative metallographyc analysis. This result has been used to estimate the thermo-mechanical properties (Young's modulus, Poisson's ratio, expansion coefficient ,thermal conductivity), using mixtures rule and micromechanics concepts.

With a linear thermo-mechanical model has been shown that:

- the porosity of sintered steel do not modify substantially the thermal distribution inside the piston, in steady state conditions
- the thermal gradient in the piston is negligible
- the thermal expansion of the piston and the deformed shape are strongly dependent on the thermo-mechanical properties related to sintered steel porosity gradient
- with a proper design, the shape distortion of the sintered steel piston can be minimized, to be similar to cast iron solution

REFERENCES

[1] Smithells Metals Reference Book, Seventh edition, Butterworth-Heinemann, 1992, pp. 14-28.

[2] W. D. Kingery, H. K. Bowen and D. R. Uhlmann " *Introduction to Ceramics*", second edition, J. Wiley & Sons, 1976, pp. 594-777.

[3] D. W. Richerson "*Modern Ceramic Engineering*", Dekker, 1982, pp. 39-76.

[4] Metals Handbook, Vol. 14, Powder Metallurgy, 9[a] ed., ASM, 1984, pp. 333, 463-478.

[5] R. M. German "*Powder Metallurgy Science*", Metal Powder Industries Federation, 1994, pp. 389-392.

[6] J. C. Y. Koh and A. Fortini, Int. J. Heat Mass Transfer, Vol. 16, 1973, pp. 2013-2022.

[7] T. W. Clyne and P. J. Withers "*An Introduction to Metal Matrix Composites*", Cambridge University Press, 1993, pp.117-123.

[8] D.R. Poirier, G.H. Geiger *"Transport Phenomena in Materials processing"* TMS 1994

[9] R. H. Perry, D.W. Green *"Perry's Chemical Engigneers' Handbook"* 7th ED. McGRAW-HILL 1997